

Tectonic stress in the Earth's crust: advances in the World Stress Map project

B. SPERNER¹, B. MÜLLER¹, O. HEIDBACH¹, D. DELVAUX^{2,3}, J. REINECKER¹
& K. FUCHS¹

¹*Geophysical Institute, Karlsruhe University, Hertzstrasse 16, 76187 Karlsruhe, Germany
(e-mail: blanka.sperner@gpi.uni-karlsruhe.de)*

²*Royal Museum for Central Africa, Leuvensesteeweg 13, 3080 Tervuren, Belgium*

³*Present address: Vrije University, Amsterdam, The Netherlands*

Abstract: Tectonic stress is one of the fundamental data sets in Earth sciences comparable with topography, gravity, heat flow and others. The importance of stress observations for both academic research (e.g. geodynamics, plate tectonics) and applied sciences (e.g. hydrocarbon production, civil engineering) proves the necessity of a project like the World Stress Map for compiling and making available stress data on a global scale. The World Stress Map project offers not only free access to this global database via the Internet, but also continues in its effort to expand and improve the database, to develop new quality criteria, and to initiate topical research projects. In this paper we present (a) the new release of the World Stress Map, (b) expanded quality ranking schemes for borehole breakouts and geological indicators, (c) new stress indicators (drilling-induced fractures, borehole slotter data) and their quality ranking schemes, and (d) examples for the application of tectonic stress data.

Tectonic stress is felt most extremely during its release in catastrophic earthquakes, although less spectacular tectonic stress is a key safety factor for underground constructions such as tunnels, caverns for gas storage or deposits of nuclear waste (Fuchs & Müller 2001). Furthermore, the economic aspect is of increasing importance in hydrocarbon recovery. Knowledge of the stress field is used in the hydrocarbon industry to foresee stability problems of boreholes and to optimize reservoir management through tectonic modelling in combination with correlation with other data sets such as 3D-structural information, e.g. location and orientation of faults.

Geodetic measurements (e.g. Global Positioning System, GPS; Very Long Baseline Interferometry, VLBI; Satellite Laser Ranging, SLR) have become available in increasing numbers and enhanced quality. They provide surface displacement vectors from which the strain rate field can be deduced. The combined interpretation of stress and strain rate data provides unique challenges for Earth scientists in a number of fields. In tectonics, plate boundary forces confine the kinematics of plate motion and the dynamics of plate deformation resulting, for example, in major differences between intraplate and plate boundary deformation zones. The width of the latter even varies for the

different types of plate boundaries (Gordon & Stein 1992). These differences express the laterally and vertically heterogeneous deformation pattern of the crust due to its composition, mechanical properties and tectonic setting. The comparison of the strain rate field at the surface with earthquake data from the seismogenic part of the crust will give information on the depth variation of strain. The relationship of strain and stress is of special importance at active fault zones, where accumulated stress is abruptly released in earthquakes.

The scale of stress impact ranges from a continent-wide scale in order to explain tectonic processes, to a metre scale at reservoir and construction sites. The global database World Stress Map (WSM) provides information on the contemporary tectonic stress in the Earth's crust in a compact and comprehensive way. The WSM project was initiated as a task force of the International Lithosphere Program under the leadership of M. L. Zoback. The database is now maintained and expanded at the Geophysical Institute of Karlsruhe University as a research project of the Heidelberg Academy of Sciences and Humanities. The WSM team regards itself as 'brokers' for these fundamental data: data of different types from all over the world are integrated into a compact database following standardized procedures for quality assign-

ment and for data format conversion. The resulting database is available to all via the Internet (<http://www.world-stress-map.org>) for further investigations.

We are indebted to numerous individual researchers and working groups all over the world for providing data for the database and we are looking forward to receiving new data for upgrading the database in the near future. For its successful continuation the WSM project is dependent on further data release from industry and academia.

Since the presentation of the WSM project in a special volume of the *Journal of Geophysical Research* in 1992 (Vol. 97, no. B8), relevant changes took place, not only concerning the amount of data available in the WSM database, but also regarding new methods for stress investigations (e.g. drilling-induced fractures, borehole slotter) as well as improved quality criteria for geological indicators and for borehole breakouts. Here, we give an overview about the state-of-the-art of the database complemented by an outlook on the capability of stress data for practical applications in industry and academia. Thereby, we concentrate on the new features of the WSM; for basic information about the project we refer readers to the *Journal of Geophysical Research* special volume (as mentioned above).

Database and Internet access

Information about the tectonic stress field in the Earth's crust can be obtained from different types of stress indicators, namely earthquake focal mechanisms, well bore breakouts, hydraulic fracturing and overcoring measurements, and young (Quaternary) geological indicators like fault-slip data and volcanic alignments. The reliability and comparability of the data are indicated by a quality ranking from A to E, with A being the highest quality and E the lowest (for further investigations only the most reliable data with a quality of A, B or C should be used). An overview about the quality ranking scheme is given in Zoback (1992) as well as on the WSM website (<http://www.world-stress-map.org>).

The WSM website gives a detailed description of the database comprising not only data on the orientation of the maximum horizontal compression (S_H), which are usually plotted on the stress maps, but also information such as the depth of the measurement, the magnitude, the lithology and so on. The complete database can be downloaded from the website either as dBase IV or as an ASCII file. In addition, the website provides instructions for stress regime characterization, abstracts from the two WSM Euroconferences, interpretations of the stress field in selected

regions, guidelines for data analysis (which until now are available for borehole breakouts), and much more.

Numerous stress maps for different regions of the world are available on the Internet as postscript files. As an additional service the program CASMO (Create A Stress Map Online) offers the possibility to create user-defined stress maps, for example by adding topography, plotting only data of a specific type (e.g. only earthquakes), or plotting data from a certain depth range. CASMO is available on request and takes less than two hours for a return of the stress map via e-mail. All stress maps are plotted with GMT provided by Wessel & Smith (1991, 1998; <http://www.soest.hawaii.edu/gmt/>); plate boundaries come from the PLATES project (<http://www.ig.utexas.edu/research/projects/plates/plates.html>).

The new release of the WSM

The new release of the WSM (Müller *et al.* 2000; Fig. 1) encompasses 10 920 data records, each with up to 56 detail entries. As in the earlier releases (e.g. Zoback 1992; Müller *et al.* 1997) most data come from earthquakes (63%; with Harvard University being the major 'data contributor'; CMT solutions; <http://www.seismology.harvard.edu/projects/CMT/>) and borehole breakouts (22%; Table 1, Fig. 2). About two-third of the data (68%) have a quality of A, B or C and thus can be used for further investigations (D and E quality data are too unreliable, but are kept for book-keeping purposes in order to inform future researchers that these data have already been analysed). New data mainly came from Europe, Australia and America.

The WSM database is designed as a tool to work with stress data. Due to the structure of the database the data can be selected according to a number of criteria such as type, location, regime, depth, and so on. Additionally, data from mid-ocean ridges which may be directly related to plate boundary processes and which had so far been excluded from the WSM database are now included. These data with less than 2° distance to the next plate boundary are marked by 'PBE' (Possible Plate Boundary Event) in the last field of the database (field PBE), so that they can easily be filtered if necessary.

New database structure

A three-letter country code is used for the numbering of the data; it is based on ISO 3166 provided by the United Nations (<http://www.un.org/Depts/unsd/methods/m49alpha.htm>). We opted for a new

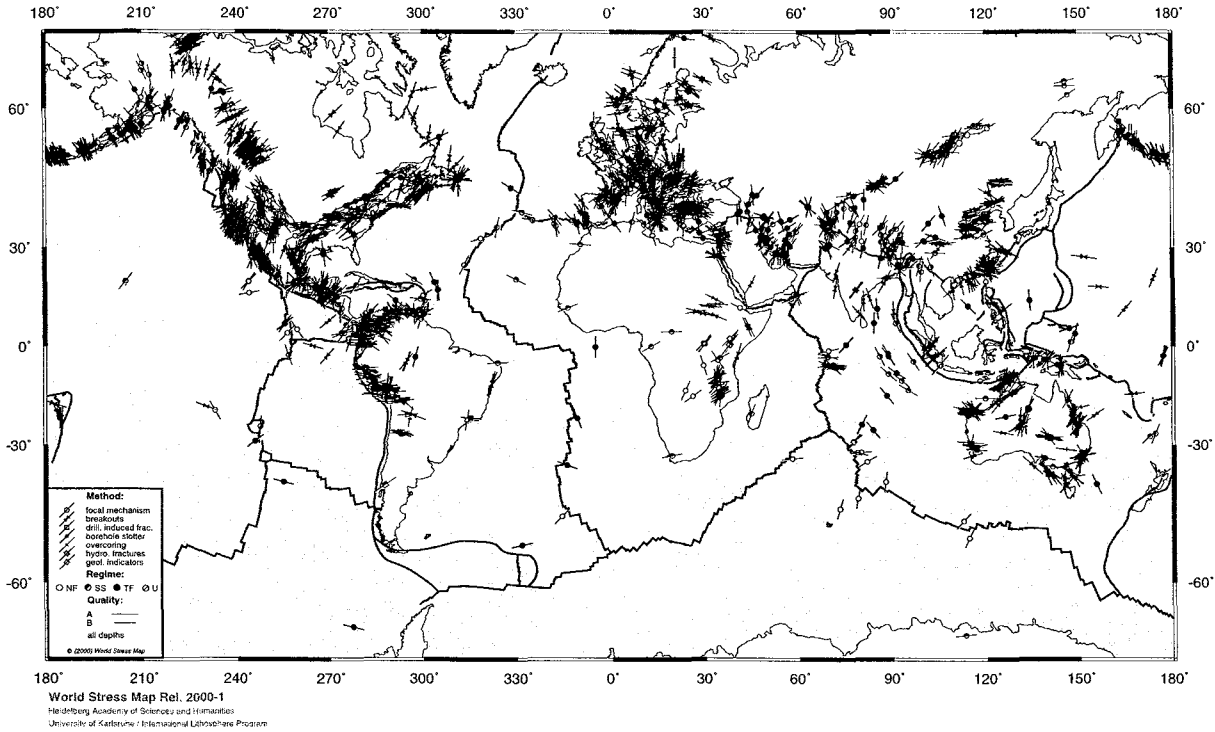


Fig. 1. The new release of the World Stress Map (WSM 2000). Lines show the orientation of the maximum horizontal compression (S_H); different symbols represent different data types, different symbol sizes characterize different data qualities; different colours and fillings indicate different stress regimes (red/unfilled, normal faulting (NF); green/half-filled, strike-slip faulting; (SS); blue/filled, thrust faulting (TF); black, unknown (U)).

Table 1. Distribution of data types in the WSM database

Data type (abbreviations)	Number (A–E)	Percentage	Number (A–C)	Percentage
Focal mechanism (FMS, FMA, FMC)	6893	63.12	4894	66.30
Borehole breakouts (BO, BOC, BOT)	2414	22.11	1683	22.80
Geological: fault-slip (GFI, GFM, GFS)	373	3.42	321	4.35
HydroFrac (HF, HFG, HFM, HFP)	314	2.88	205	2.77
Overcoring (OC)	615	5.63	104	1.41
Geological: volcanic alignments (GVA)	223	2.04	101	1.37
Drilling-induced fractures (DIF)	44	0.40	36	0.49
Borehole slotter data (BS)	33	0.30	29	0.39
Petal centreline fracture (PC)	9	0.08	9	0.12
Shear wave splitting (SW)	2	0.02	0	0
Sum:	10920	100.00	7382	100.00

For details about the data types see <http://www.world-stress-map.org>

country code to eliminate confusion occurring with the old country code. The latter subdivided some countries into several (tectonic) units. However, this subdivision was not done consistently (some countries like Mexico were subdivided into numerous subunits, while other large countries were not subdivided) we decided for the option one country = one code according to international standards. Information about the tectonic unit can be given/found in the fields 'LOCALITY' or 'COMMENT'. For the same reasons, the oceans are no

longer subdivided into different regions, but all get the code 'SE'. The three-letter country code is noted in the new field 'ISO' at the very beginning of each data record; the field 'SITE' with the old numbering remains part of the database to guarantee the comparability with older releases. To avoid the millennium bug (Y2K problem) all fields containing a date, i.e. the fields 'DATE', 'REF1' to 'REF4', and 'LAST—MOD', were extended by two characters and the year is now shown as four-digit number.

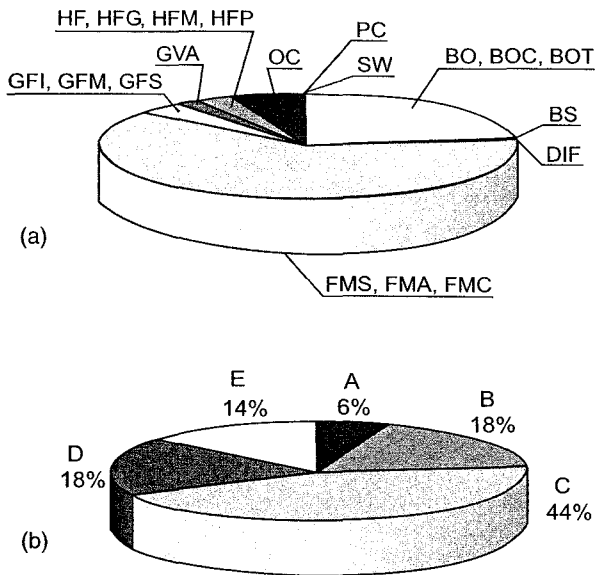


Fig. 2. Distribution of the WSM 2000 data with respect to (a) data type (see Table 1 for abbreviations) and (b) quality (A, best, E, worst quality). Most data come from earthquakes (63%; FMS, FMA, FMC) and borehole breakouts (22%; BO, BOC, BOT). The most frequent quality is C due to the fact that most earthquake data are Harvard CMT solutions which are assigned quality C (for discussion see Zoback 1992).

New quality ranking schemes

During the operation of the WSM database and from discussion with other researchers, the original quality ranking schemes have been modified and improved. This is sometimes related to clarity of the quality assignment instructions and sometimes to the use of different tools for recording of the data. Up to now, the modification is complete for three types of stress indicators, geological indicators (especially fault-slip data), borehole breakouts, and overcoring data. Others will follow.

Expanded quality ranking scheme for geological indicators (GFI, GFM, GFS)

Many methods for analysing fault-slip data (e.g. Allmendinger *et al.* 1989; Angelier 1984) and numerous computer programs have been developed

(e.g. Sperner *et al.* 1993; Sperner 1996; Delvaux *et al.* 1997). Nevertheless, some disagreement prevails concerning the meaning of the determined orientations, whether they represent strain rate or stress orientations; for a review see Twiss & Unruh (1998). We do not intend to interfere with that discussion or to describe all these methods and the related software. Instead we want to provide a useful tool for quality ranking.

Quality ranking for fault-slip data has so far been defined through the following criteria:

A quality: inversion of fault-slip data for best fitting mean deviatoric stress tensor using Quaternary age faults (GFI data).

B quality: slip direction on fault plane, based on mean fault attitude and multiple observations of the slip vector; maximum stress at 30° to fault (GFM data).

C quality: attitude of fault and primary sense of slip known, no actual slip vector (GFS data).

D quality: (a) offset core holes, (b) quarry pop-ups, or (c) postglacial surface fault offsets.

Due to this quality ranking GFI data (inversion of fault-slip data) are *always* assigned quality A. However, the quality of these data is dependent on several different criteria such as the number of data and the average misfit between calculated and theoretical slip direction. We use these criteria to introduce a new quality ranking for GFI data. For each of these criteria 'subqualities' ranging from 'a' to 'e' are defined (Table 2). The overall quality of the analysis is given by its *lowest* subquality.

Quality criteria for GFI data

(a) *Number of data.* The number of data used for the calculation of the stress axes.

(b) *Percentage of data.* The percentage of data relative to the total number of data measured in an outcrop. With more than one event recorded in an outcrop, the quality will (in most cases) decrease reflecting the difficulty to correctly separate the data into subsets.

(c) *Confidence number.* The reliability of the results of fault-slip analysis is very sensitive to the

Table 2. *Quality ranking scheme for fault-slip data (GFI)*

Subquality	Number of data	Percentage of data	Confidence number (slip sense determ.)	Fluctuation (°) (average misfit)	Data type
a	≥25	≥60	≥0.70	≤9	≥0.90
b	≥15	≥45	≥0.55	≤12	≥0.75
c	≥10	≥30	≥0.40	≤15	≥0.50
d	≥6	≥15	≥0.25	≤18	≥0.25
e	<6	<15	<0.25	>18	<0.25

The overall quality is defined by the *lowest* subquality of any of these criteria.

reliability of slip sense determination. Hardcastle (1989) introduced four confidence levels (1–4) for slip sense determination which are assigned to the single faults during field measurements. We gave these confidence levels different weights in the following way:

1, absolutely certain:	1.00
2, certain:	0.75
3, uncertain:	0.50
4, very uncertain or unknown:	0.25

The 'confidence number' is defined as the average of these values for all data used in the final analysis. If no confidence levels were assigned during field measurements the overall quality assigned due to the 'rest' of the criteria is taken and downgraded by one class (e.g. from quality B to C).

(d) *Fluctuation*. The fluctuation is defined as the arithmetic mean between the measured and the theoretical slip directions (the theoretical slip direction is assumed to be parallel to the direction of maximum shear stress along the fault plane).

(e) *Type of data*. Information from other structures like tension joints can give additional constraints on the calculated stress tensor. The computer program TENSOR written by Delvaux (Delvaux *et al.* 1997; Delvaux & Sperner 2003) includes these data into the stress analysis by using different weights for the different types of structures:

Slickenside	1.00
Tension/compression joint	0.50
Two conjugated planes	0.50
Movement plane + tension joint	0.50
Shear joint	0.25

The average value for all structures used in the stress analysis gives the 'data-type number' for Table 2. For pure fault-slip data sets this number (1.00) has no relevance.

(f) *Diversity of orientation of fault planes and of lineations*. Fault-slip analysis is based on an equation system with four unknowns (Angelier & Goguel 1979) due to the search for the orientation of the three stress axes and for the stress ratio. Thus at least four differently oriented fault planes are necessary to reveal an unambiguous result. Unbalanced data sets with fault planes and lineations with similar orientations will not give clear results for both the orientation of the stress axes and the stress ratio. Data sets including only two fault plane orientations (conjugated fault sets) give better, but still not optimum restrictions concerning the stress axes, while the stress ratio is still undefined. Thus, the diversity of the measured data ensures the non-ambiguity of the calculated result. A measure of the diversity is given by the normalized length of the mean vector of the fault plane

poles and of the mean slip line vectors. This normalized length is close to 1 for parallel planes or parallel lineations and could be used as an additional quality criterion. But in contrast to the other quality criteria (which are all standard measures in fault-slip analysis) the diversity cannot be easily obtained from published data. It can only be estimated from the data plots, but for an accurate calculation the original data must be available in digital form. Thus, we gave up our initial intention to include the diversity into the quality ranking, but we plead for a careful handling of fault-slip data concerning this problem. Data sets which show a clearly unbalanced fault plane orientation might be downgraded by the WSM authorities.

In this context the quality ranking of two other geological indicators, i.e. GFM and GFS data (see definition above), has to be critically reviewed. Their quality assignment is justified for recently active, large-scaled structures as described by Zoback (1992), i.e. for earthquake fault scarps. But the fact that these data build one data class together with GFI data (fault-slip inversion; see above), which are derived from microstructures, brings the danger that small-scaled structures are used in the same way. In this case, the GFM and GFS data are downgraded to quality C and D, respectively (Table 3); the motivation for this is given in the following paragraphs.

GFM data are derived from single fault planes under the assumption of an angle of 30° between maximum compression axes and fault plane (with the fault plane pole, the lineation and the compression axis lying in one plane). For newly formed faults, e.g. in Quaternary rocks, this assumption might be reasonable, but for reactivated faults other angles are as probable as the usually taken 30° (e.g. San Andreas Fault with *c.* 80°; Zoback *et al.* 1987). This uncertainty makes it necessary to downgrade data of this type to quality C, instead of B as in the old quality ranking scheme. This is additionally justified when taking into account that data from fault-slip inversion (GFI data) with quality B are based on at least 15 fault-slip data with an average misfit angle less than 12°. GFM data do not reach this level of accuracy and thus represent a lower quality (i.e. quality C).

The next lower level of quality is represented by GFS data which are derived from fault planes with

Table 3. Additional constraints for the quality ranking of GFM and GFS data

Data type	GFM	GFS
Large scale (earthquake related)	B	C
Small scale (microstructures)	C	D

unknown slip vector, but with 'primary sense of slip known' (due to the old quality ranking scheme). Usually this 'primary sense of slip' is derived from the offset of planar structures (e.g. bedding planes). As long as no other planar structure, oblique to the first one, gives additional information on the slip direction, no statement about the slip direction can be made. The offset of one-dimensional features (e.g. longish fossils) gives an unambiguous indication for the slip direction, but they are rarely found offset in nature. Thus, the offset along a fault usually does not clearly show the slip direction from which to derive the orientation of the principal stress axes. Consequently we downgraded the quality assignment for this type of data (GFS data) to quality D.

Expanded quality ranking scheme for borehole breakouts (BO, BOC, BOT)

Breakouts develop when the stress concentration at the borehole wall exceeds the rock strength. They occur in the direction of the minimum horizontal stress S_h , 90° off the orientation of the maximum horizontal stress S_H . In the last two decades of breakout investigation logging tools have improved and the horizontal as well as the vertical resolution of the recorded data have increased. A variety of breakout interpretation methods based on these high resolution tools have been developed. To assist the individual researcher and to keep data comparable the WSM team set up guidelines of data analysis for borehole breakout investigation.

(a) *Criteria for breakout identification.* Numerous authors have treated the problem of breakout identification (e.g. Fordjor *et al.* 1983; Plumb & Hickman 1985; Peska & Zoback 1995; Zajac & Stock 1997). For the WSM database we suggest the following criteria for the identification of breakouts from borehole geometry tools such as BGT, SHDT, FMS, FMI. These criteria are modified after Plumb & Hickman (1985) and Zajac & Stock (1997).

- (1) Tool rotates freely below and above the breakout interval. Rotation has to stop in the breakout interval.
- (2) Caliper difference has to exceed 10% of bit size.
- (3) The smaller caliper has to range between bit size and 110% of bit size.
- (4) The length of the breakout zone has to be at least 1 m.
- (5) The direction of elongation must not consistently coincide with the azimuth of the high side of the borehole. Thus, for boreholes which deviate more than 1° from vertical, the angular difference between the direction of

the hole azimuth and the azimuth of the greater caliper has to exceed 15° .

(b) *Recommendations for breakout analysis*

- (1) Use breakout identification criteria (see above).
- (2) Use visual control (for caliper data): if the analysis is purely based on the statistics of Pad-1 azimuth (Fig. 3a), direction A would

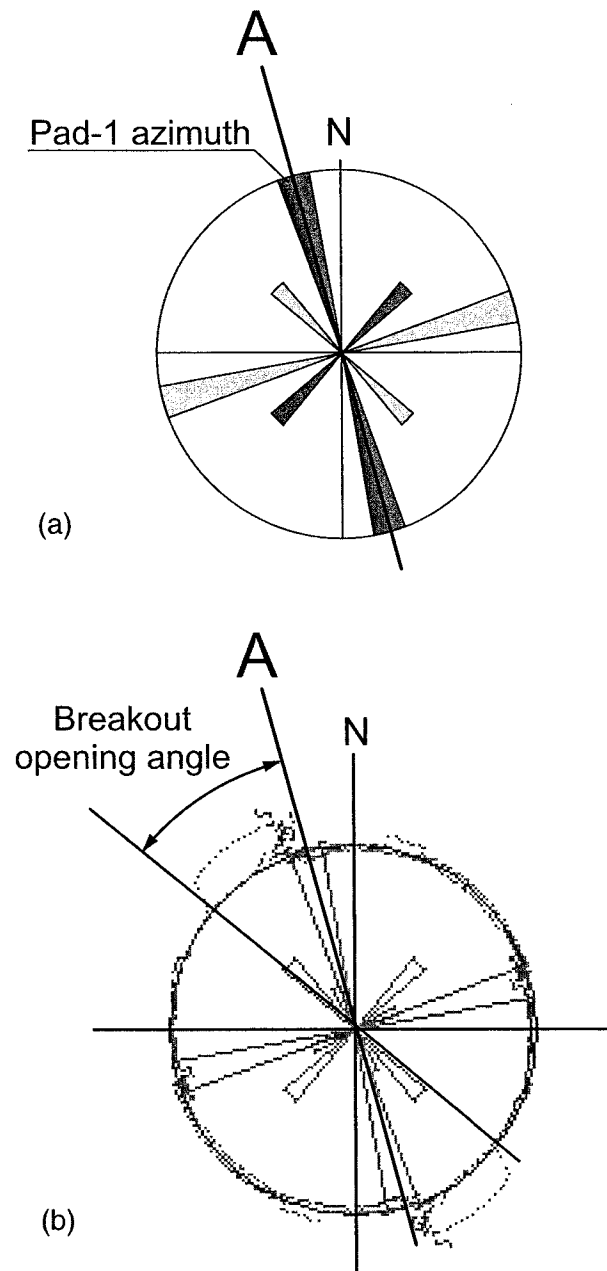


Fig. 3. (a) Distribution of four-arm caliper data (Pad-1,3 azimuth: dark grey; Pad-2,4 azimuth: light grey). Due to the Pad-1,3 maximum orientation 'A' seems to represent the breakout orientation. (b) Contour plot of caliper data. The distribution of the data indicates that the tool stuck to one side of the breakout (due to cable torque), so that orientation 'A' does not represent the correct breakout azimuth.

be obtained as breakout azimuth. But, due to cable torque, the tool may stick to one side of the breakout and A may be off the true breakout azimuth. Contour plots help to avoid this source of error (Fig. 3b).

- (3) Use circular statistics (e.g. Mardia 1972).
- (4) Correct the S_H azimuth according to magnetic declination at the time of logging.
- (5) Check for key seats: a means to check for key seat effects is to plot breakout orientation with depth including the direction of hole azimuth (Fig. 4).

(c) *Quality ranking scheme for borehole breakouts.* For borehole breakouts the quality is ultimately linked to the standard deviation, the number

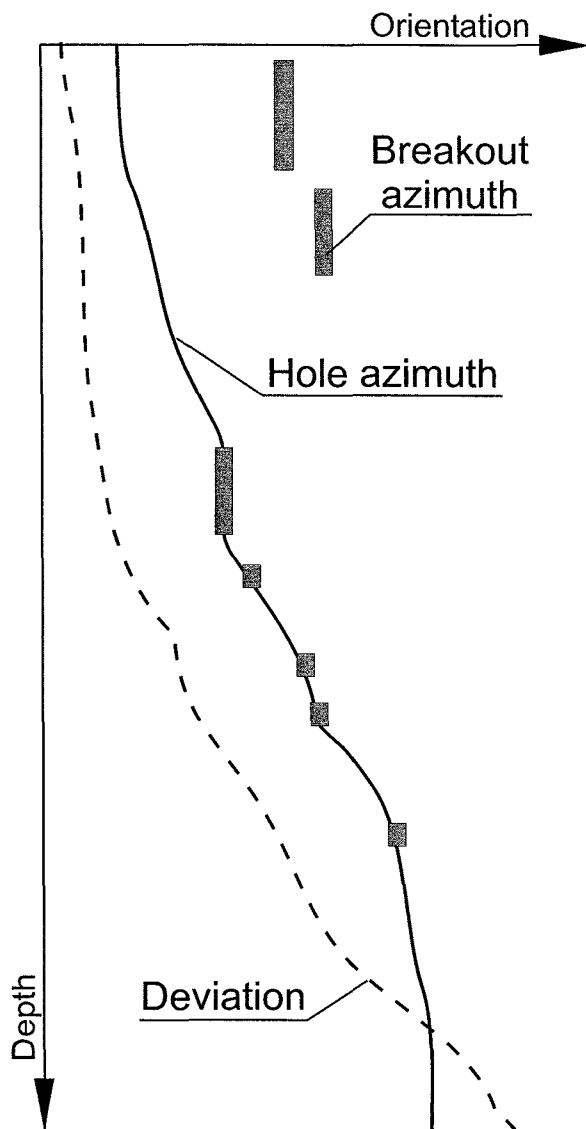


Fig. 4. Identification of key seats. In the deeper section the breakouts follow the direction of the hole azimuth indicating possible key seats. Deviation: angle between borehole and vertical direction; hole azimuth: dip azimuth of non-vertical borehole.

of breakouts and the total length of breakouts (Zoback 1992) (Table 4). The overall quality of the analysis is given by its *lowest* subquality.

Expanded quality ranking scheme for overcoring data (OC)

The previous quality ranking for overcoring measurements contained some unclear formulations (e.g. 'multiple consistent measurements') which will be removed. For the sake of consistency, overcoring data will be treated like borehole slotter data because they face similar problems in quality ranking. (For details see section on Borehole slotter data and Table 6.)

New methods

Two new types of stress indicators are now included in the WSM database: drilling-induced fractures (DIF) and borehole slotter data (BS). Their quality rankings are described in detail below.

Drilling-induced fractures (DIF)

The availability of high resolution logging tools such as FormationMicroScanner (FMS), FormationMicroImager (FMI) or Borehole Televiwer (BHTV) enables the analysis of tensile failure phenomena at the borehole wall. In the WSM database tensile failure from induced hydraulic testing (hydrofrac) is already included. In addition to the stimulated hydrofracs, unintentional tensile failure created during drilling may occur (Fig. 5a). These drilling-induced fractures (DIF) can be used for stress determination (Wiprut *et al.* 1997; Fig. 5b). Identification criteria have been proposed, for example by Brudy & Zoback (1999) and Ask (1998). We basically follow their criteria with some minor modifications.

Table 4. *Quality ranking scheme for borehole breakouts (BO, BOC, BOT)*

Subquality	Number of data	Total length (m)	Standard deviation (°)
a	≥ 10	≥ 300	≤ 12
b	≥ 6	≥ 100	≤ 20
c	≥ 4	≥ 30	≤ 25
d	< 4	< 30	≤ 40
e	-	-	> 40

The overall quality is defined by the *lowest* subquality of any of these criteria.

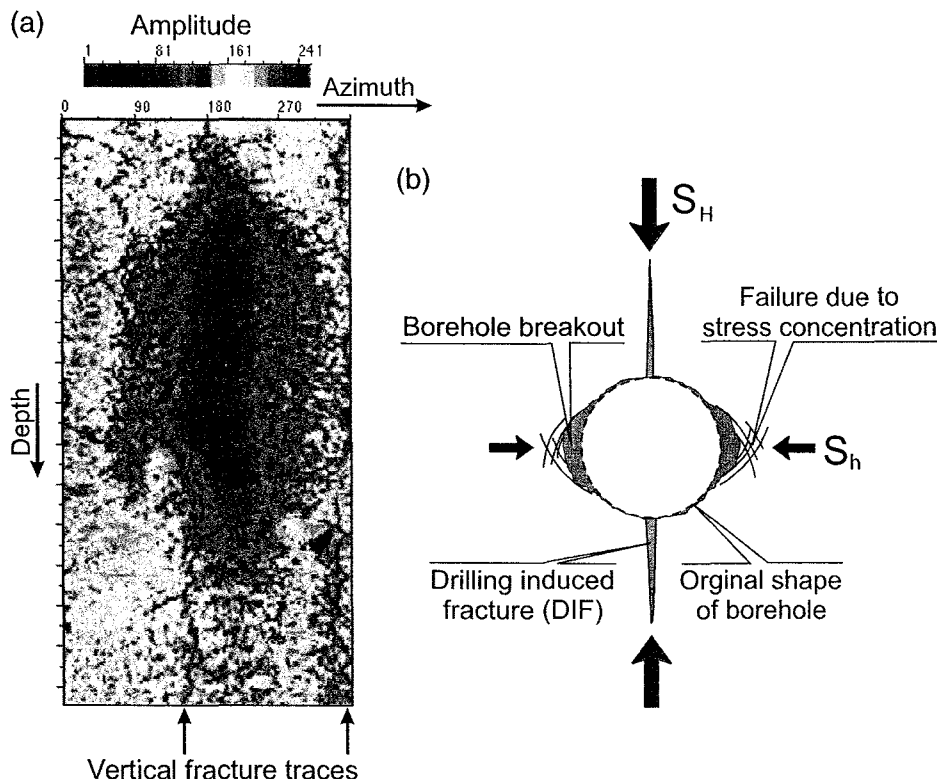


Fig. 5. (a) Borehole televiwer image with vertical fracture traces which are interpreted as drilling-induced fractures. Colours correspond to the amplitude of the reflected acoustic (ultrasonic) pulse and thus to the reflection coefficient of the borehole wall (low amplitude = rough, fractured borehole wall such as in breakout intervals). (b) Sketch of a borehole with drilling-induced fractures parallel to the maximum horizontal compression (S_H) and borehole breakouts perpendicular to S_H .

(a) *Criteria for DIF identification*

- (1) Fractures that are subparallel to the borehole axis, occur in pairs on opposite sides of the borehole wall and are not connected to each other (not to be misinterpreted as sinusoidal steep fractures).
- (2) Short en-echelon fracture traces (also occurring in pairs) but inclined with respect to the borehole axis. They result from stress distribution at the borehole wall when the borehole axis does not coincide with one of the principal stress axes.
- (3) The length of DIFs ranges between 0.1 and 2 m.
- (4) If breakout observations are available DIF and breakout orientations should differ by 90° .
- (5) The shape of DIFs should be irregular since perfectly straight features could result from mechanical wear of the borehole.

(b) *Quality ranking scheme for DIFs.* The quality ranking scheme for DIFs is based on the number of fractures which had been identified, the standard deviation of their average and the total fracture length (Table 5). The quality ranking scheme is similar in structure to the breakout quality ranking.

Borehole slotter data (BS)

Borehole slotter data are obtained by a stress relief method (no overcoring) which is described in detail by Bock & Foruria (1983), Bock (1993), and Becker & Werner (1994). Results of borehole slotter measurements agree with data from other methods (e.g. borehole breakouts; Becker & Werner 1994). Becker & Paladini (1990) developed a quality ranking scheme for *in situ* stress data which we used as a basis for the (new)

Table 5. *Quality ranking scheme for drilling induced fractures (DIF)*

Subquality	Number of data	Total length (m)	Standard deviation ($^\circ$)
a	≥ 10	≥ 300	≤ 12
b	≥ 6	≥ 100	≤ 20
c	≥ 4	≥ 30	≤ 25
d	< 4	< 30	≥ 40
e	< 4	< 30	> 40

The overall quality is defined by the *lowest* subquality of any of these criteria.

Table 6. *Quality ranking scheme for borehole slotter (BS) and overcoring (OC) data*

Subquality	Number of data	Depth of measurement (m)	Standard deviation (°)
a	≥11	≥300	≤12
b	≥8	≥100	≤20
c	≥5	≥30	≤25
d	≥2	≥10	≤40
e	<2	<10	>40

The overall quality is defined by the *lowest* subquality of any of these criteria.

WSM quality ranking. We adapted it to the already existing criteria for similar stress indicators like overcoring or breakout data. Important criteria are the depth of measurement, the number of data and the standard deviation of the principal stress axes orientation (Table 6). Borehole slotter measurements normally are within the first 30 m of a borehole, so that topographic effects or stress deflections around underground openings might influence the result. Thus the distance to topographic features (e.g. quarry walls) and excavation walls in the case of underground openings is important: the distance to topographic features must be larger than three times the height of the topographic feature and the distance to excavation walls must be larger than two times the excavation radius (Fig. 6). All measurements at smaller distances are assigned quality E.

Quality assignment and depth of measurement

We are aware that the quality assignment cannot be transferred from one method to another. Researchers may argue that the assignment of qualities A or B to borehole slotter (BS) or overcoring (OC) data is restricted to measurements at depths greater than 100 m, which is in most cases equal-

ent to measurements in tunnels or mines since the drillholes for BS and OC data usually are less deep. In contrast to borehole slotter and overcoring data, the quality ranking for geological fault-slip data (GFI), drilling-induced fractures (DIF), and borehole breakouts (BO) does not contain such a depth criterion. For the latter two it is considered to be unnecessary because these data result from measurements in industrial wells at several hundred metres depth. In addition, the depth condition for BOs and DIFs is substituted by the conditions of total length of BO or DIF data, respectively.

GFI data are surface data in terms of measurements. However, their origin may be from greater, but unknown, depth. To account for the missing depth condition in the quality ranking of the GFI data a larger number of data is required. For example, quality A can be obtained with a minimum of 25 data for GFI measurements, while only 11 are needed for BS and OC measurements.

Application of tectonic stress data

Numerous fields of applications exist for tectonic stress data. They are not restricted to pure ‘academic’ research projects, but also include investigations with large economic impact, e.g. in hydrocarbon or geothermal energy production. In the following we give examples for both types of application. For the ‘academic’ example we selected the eastern Mediterranean region where numerous stress data are available and where geodetic measurements (GPS, SLR) provide the possibility to compare both data sets. The ‘economic’ examples deal with the stability of underground openings and with hydrocarbon reservoir management.

Stress and velocity in the eastern Mediterranean region

Tectonic overview The Neogene to recent tectonic evolution of the eastern Mediterranean region is driven by the north–south convergence between the African and Arabian plates, and the Eurasian plate.

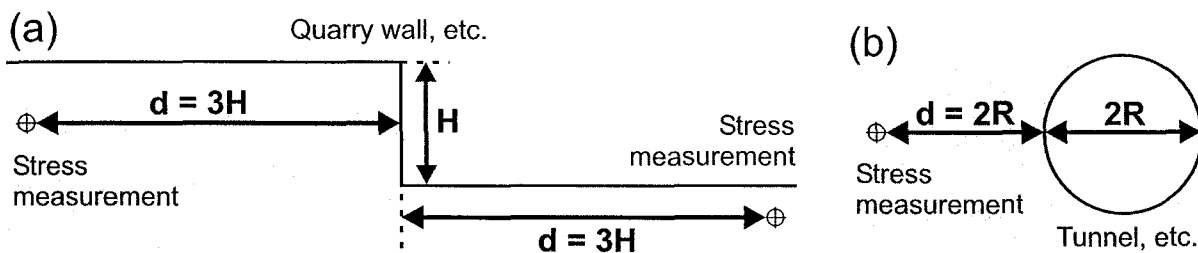


Fig. 6. Minimum distance *d* of stress measurements from (a) topographic features (three times the height of the topographic feature) and (b) underground openings (two times the excavation radius).

The African plate moves at a velocity of 9 mm a^{-1} and the Arabian at 25 mm a^{-1} relative to the Eurasian plate (DeMets *et al.* 1994). An assemblage of lithospheric blocks trapped in this convergence zone moves independently between Africa, Arabia and Eurasia resulting in oblique continental collisions and thus in the close vicinity of collision and subduction zones (e.g. McKenzie 1972). Subduction occurs beneath the Hellenic Arc, while continental collision already started in its lateral continuations towards the NW (Dinarides) and towards the east (Cyprean Arc) (Fig. 7). The southwestward retreat of the Hellenic Arc subduction zone causes backarc extension in the Aegean and enables the westward extrusion of the Anatolian block out of a zone of continental collision at the eastern end of the Anatolian block (e.g. McKenzie 1970; Le Pichon & Angelier 1979; Royden 1993). This collision is the result of the north-northwestward movement of the Arabian plate which is separated from the African plate by the Dead Sea fault and the Red Sea rift.

Stress data The majority of the stress data comes from fault-slip analysis (for a compilation see Mercier *et al.* 1987) and from earthquake data (e.g. Jackson & McKenzie 1988). In the Aegean and

western Anatolia normal faulting is the dominant stress regime with S_H orientations trending NW to NE indicating an approximately north-south extension (Fig. 8). In the northern part of central Anatolia strike-slip faulting is the prevailing stress regime.

North-south extension in the northern Aegean Sea and western Anatolia had been interpreted to be the expression of backarc extension due to subduction zone retreat of the Hellenic Arc (e.g. Müller *et al.* 1992). The fan-shaped arrangement of S_h (minimum horizontal stress; $S_h \perp S_H$) might result from the suction force acting radially outward (i.e. southwest- to southeastward) caused by slab rollback as shown in the numerical models of Meijer & Wortel (1996). Strike-slip movements in this region and in northern central Anatolia are most probably related to the westward directed lateral extrusion of the Anatolian block with dextral movements along the North Anatolian fault (Fig. 7).

Velocity data (GPS, SLR) Geodetic observations were initiated in the mid-1980s, so that today accurate data about the velocity vectors are available for most of the observation sites (e.g. Noomen *et al.* 1996; Reilinger *et al.* 1997; Kaniuth *et al.*

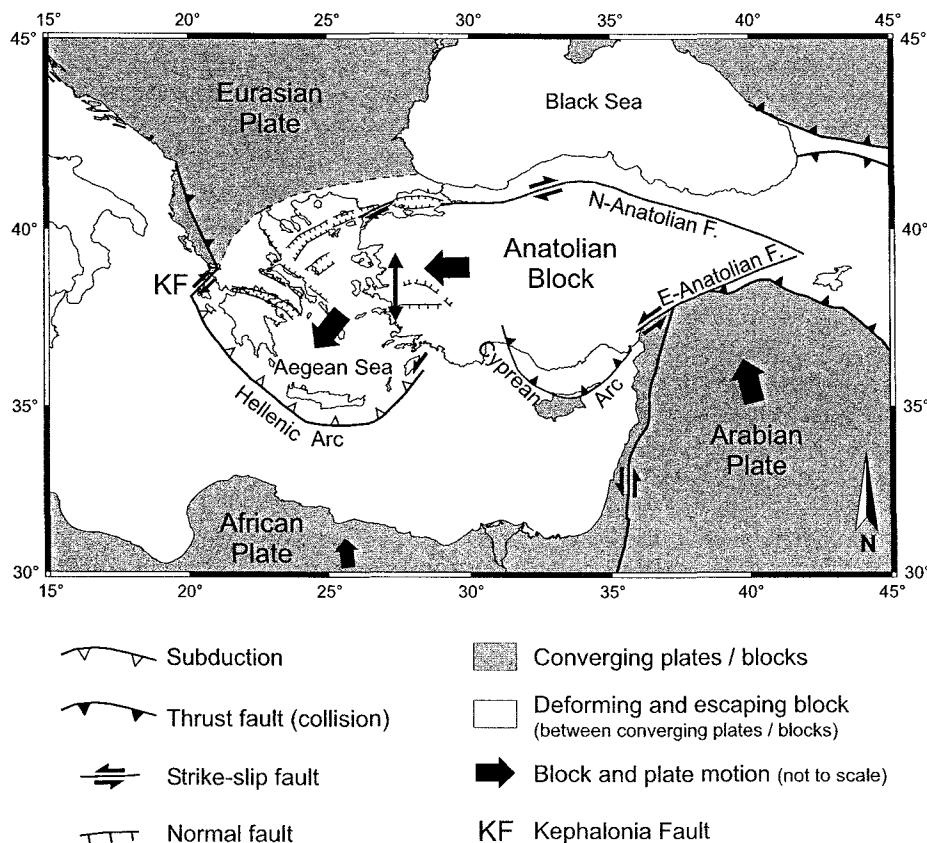


Fig. 7. Tectonic map of the eastern Mediterranean region. Lateral extrusion of the Anatolian block towards the west is triggered by continental collision of the Arabian plate with the Eurasian plate in combination with subduction zone retreat at the Hellenic arc.

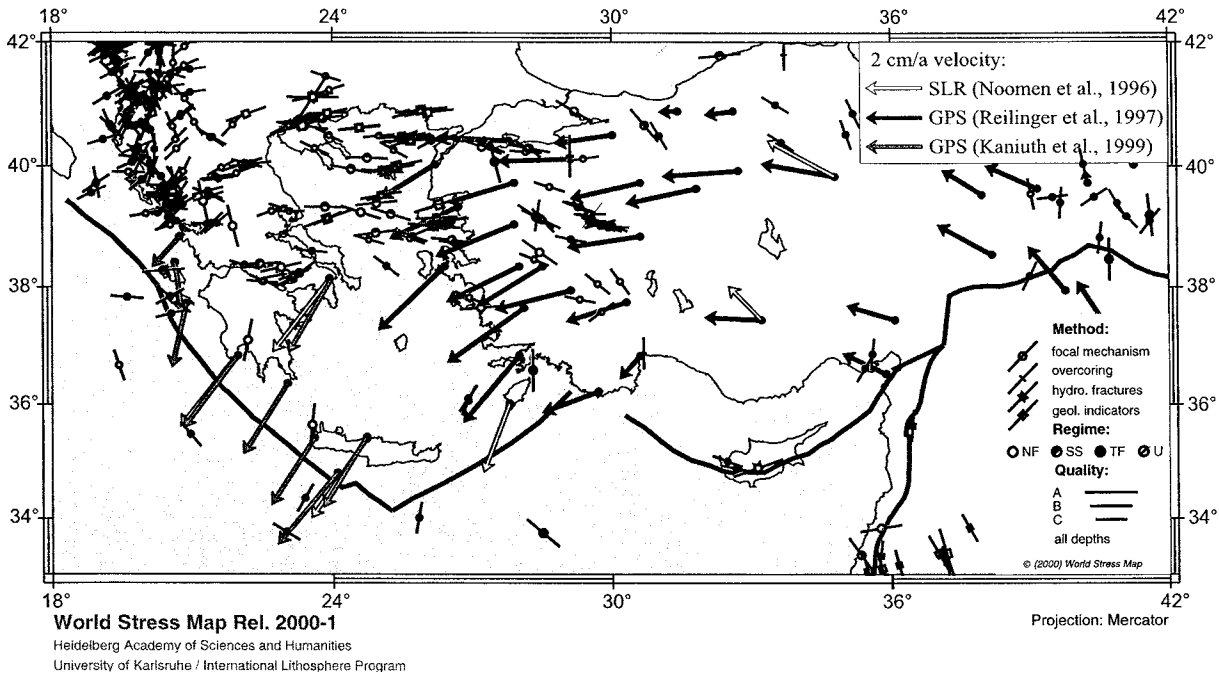


Fig. 8. Velocity and stress data for the eastern Mediterranean region. GPS data come from Reilinger *et al.* (1997) and Kaniuth *et al.* (1999), SLR data from Noomen *et al.* (1996), and stress data from the World Stress Map database (Müller *et al.* 2000). For further explanations of the stress symbols see Figure 1.

1999; Fig. 8). They indicate west-directed movements of Anatolia and southwestward movements of the Aegean. The transition zone between both blocks (western Turkey) is characterized by west-southwestward movements. The influence of plate boundary forces and different material properties on these movements have been investigated by finite element modelling. For details and references see Heidbach & Drewes (2003). Other models reconstructing the velocity vectors in the eastern Mediterranean assume two individually moving rigid lithospheric blocks: (1) the clockwise rotating Aegean block encompassing the southern and central parts of the Aegean and the southern part of Greece (south of the Gulf of Corinth); and (2) the counterclockwise rotating Anatolian block which is bordered by the North and East Anatolian faults (Fig. 7; e.g. Drewes 1993; Le Pichon *et al.* 1995). This approach fits with palaeomagnetic data which also show opposite rotation senses for both blocks (e.g. Kissel *et al.* 1987; Kissel & Laj 1988). In contrast Reilinger *et al.* (1997) modelled their set of velocity vectors with a single Aegean-Anatolian block. In general a good agreement exists, but significant discrepancies occur in western Anatolia and the southern Aegean.

Comparison of stress and velocity data For the eastern Mediterranean both types of data are explained by identical processes (see above). Nevertheless, there is no straightforward relation between them and a number of aspects have to be

taken into account when comparing stress and velocity data.

(1) Velocity fields reflect not only strain (i.e. internal deformation), but also translation and rotation (some people use the expression 'strain' in a wider sense including translation and rotation, but in this paper we use it in the more rigorous way which excludes these two processes and is restricted to distance changes between the points of a body). Thus, first rigid body movements have to be removed. For large-scale velocity fields, which have to take into account the curvature of the Earth, all rigid plate or block movements are rotations around a Euler pole. Accordingly, Reilinger *et al.* (1997) calculated the internal deformation of the eastern Mediterranean from geodetic data and found that it is small in central Anatolia. In contrast, the plate and block boundaries are characterized by broad deformation zones.

(2) Axes of principal strain rate and stress are only in some cases parallel to each other (coaxial deformation, e.g. pure shear); in most cases they are oriented obliquely to each other (non-coaxial deformation, e.g. simple shear). Additionally, the relationship between stress and strain rate might be non-linear (e.g. strain hardening or softening).

(3) Stress data are compiled throughout the whole crust while geodetic data exclusively reflect surface movements. Decoupling between different layers might result in different orientations of stress axes at different depths (e.g. Brereton & Müller 1991; Jarosinski 1998). In the eastern Mediter-

anean S_H orientations from the seismogenic upper 15 km of the crust are in good agreement with S_H orientations from the numerous surface data (geological indicators; Fig. 8). In contrast, the stress regime shows a depth dependence in the central and northern Aegean: surface data indicate a normal faulting regime, while data from depths of more than 5 km show strike-slip faulting. The change from normal faulting to strike-slip faulting regime is in contradiction to the regime changes observed elsewhere with depth which are caused by increasing overburden and thus are characterized by a change from strike-slip or thrust faulting to normal faulting. One explanation could be a gravitational collapse of the thicker crust with its higher topography in the northernmost part of the Aegean towards the central Aegean with its thinner crust and its lower topography. In this case a decoupling of the southward sliding uppermost crust from the underlying rocks would be necessary.

(4) Both data types represent different time periods. While geodetic data reflect movements during the last decade or even shorter periods, stress data come from several decades (earthquake data) or even from several tens to hundreds of thousands of years (geological indicators which come from Quaternary rocks). Deformation of the Earth's crust takes place in a non-continuous way, implied, for example, by the locally observed clustering of earthquakes through time (a seismically active period is followed by an inactive period) or by progressive failure along a fault (Stein *et al.* 1997). The seismic cycle of strong earthquakes can be as long as several hundreds of years (Jackson *et al.* 1988). For the eastern Mediterranean region the majority of the stress data comes from earthquakes and geological indicators thus reflecting a much longer time period than the geodetic measurements in Figure 8 which cover the period 1988–1994 (Reilinger *et al.* 1997). Nevertheless, McClusky *et al.* (2000) found that the geodetic data for the North and East Anatolian faults are in agreement with slip rates for the last 4–5 Ma revealed from geological data. However, the data of McClusky *et al.* (2000) do not include observations *after* the Izmit earthquake in August 1999. Earthquakes have a strong effect on the velocity field even at distances of hundreds of kilometres or more depending on the magnitude of the event. For the $M_w = 8.0$ earthquake near Antofagasta (north Chile) Klotz *et al.* (1999) observed a coseismic slip of 10 cm at a distance of 300 km.

(5) The processing of geodetic data has not yet been standardized. Thus, the results depend on the choice of the reference system and of the models included into the processing. Other critical factors are the number of observation sites and the obser-

vation time. This makes a comparison of the results of different research groups difficult or even impossible. McClusky *et al.* (2000) did a compilation of GPS data for the eastern Mediterranean which encompasses more observation sites and a longer observation period (1988–1997) compared to earlier compilations by Reilinger *et al.* (1997). The differing results of these two compilations led to different interpretations of the block movements in this region. Reilinger *et al.* (1997) 'saw' only one block, the Anatolian-Aegean block, while McClusky *et al.* (2000) 'needed' two blocks, the Anatolian and the Aegean blocks, to explain the velocity vectors (see above).

Conclusions This list of 'complications' as well as the data from the eastern Mediterranean region indicate that much more extra work is necessary to understand the relationship between stress, strain and velocity, and how these parameters depend on changes in plate tectonic processes and material properties (e.g. change of viscosity due to enhanced heat flow) as well as on local influences by seismic activity. On a global scale the ILP project 'Global Strain Rate Map' under the guidance of W. Holt (SUNY Stony Brook) and J. Haines (Cambridge University) and the WSM are prerequisites for this kind of study.

Stability of underground openings

Any underground construction causes severe modifications of the initial *in situ* rock stress at the location of the site: artificial openings create fresh surfaces which modify the boundary conditions at the location of the walls (mostly zero surface stress). This leads to a spatial distortion of the stress pattern with stress accumulations around the opening. The stress redistribution for circular holes in an anisotropically stressed rock is classically described by the Kirsch equations (Kirsch 1898). Stress redistribution around tunnels and shafts has been treated analytically as well as numerically for more complicated designs (numerous examples are summarized in Amadei & Stephansson 1997).

Since rock is less stable in tension, tensile stress concentrations may open pre-existing fractures or even fracture the rock, thus increase the weathering and leading to further instability. Compressive stresses in the vicinity of underground openings can result in different kinds of rock failure, e.g. rock bursts or side-wall spalling. In boreholes the stress-induced compressive failure is called borehole breakout (Fig. 5b).

The stability of construction sites does not depend only on the rock type but also on the orientation and magnitude of the tectonic stress in combination with the design and orientation of the

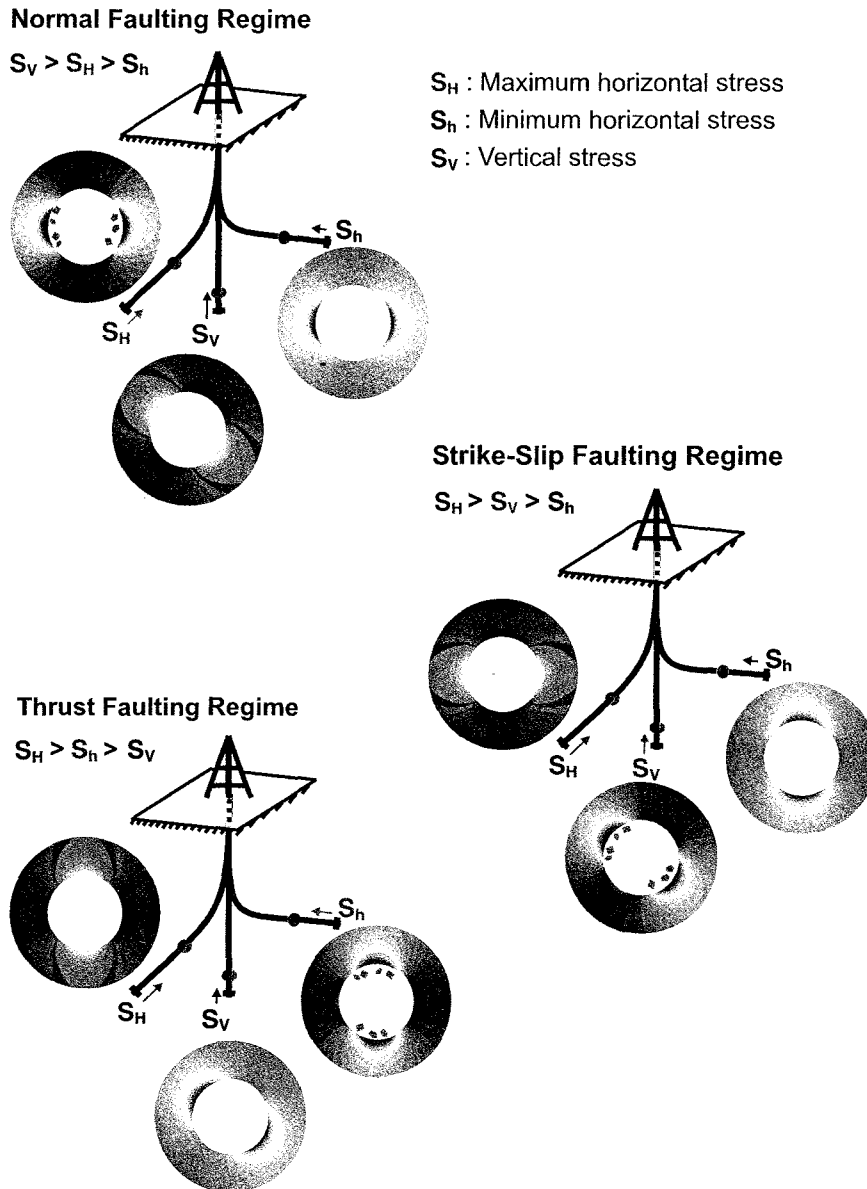


Fig. 9. Stability of underground openings due to their orientation relative to the principal stress axes. In all three stress regimes, openings parallel to the intermediate stress axis (green arrows; S_H in normal faulting, S_v in strike-slip faulting, and S_h in thrust faulting regime) are most endangered for rock failure with the failure occurring in the direction of the minimum stress axes (blue arrows; S_h in normal and strike-slip faulting, S_v in thrust faulting regime). Discs show stress concentrations (yellow to red colours) around the borehole.

underground opening. In normal faulting regimes, boreholes (shafts and mines) are most likely to fail under compression sideways when they are drilled parallel to the S_H direction (Fig. 9). This is in agreement with the observation that in places where vertical stresses are high, problems in the sidewalls of mines occur. Especially in areas with high topography and steep valley slope (for example Norwegian fjords) the tunnels that parallel the valley (parallel to S_H) show rockbursts in the tunnel wall (Amadei & Stephansson 1997). In thrust faulting regimes boreholes fail at the top and bottom if drilled parallel to S_h . Again this is in agreement with mining observations where prob-

lems in roofs and floors occur for areas of high horizontal stress. Under strike-slip conditions vertical boreholes and shafts are most endangered for failure because they experience high stress concentrations in the direction parallel to S_h .

Hydrocarbon reservoir management

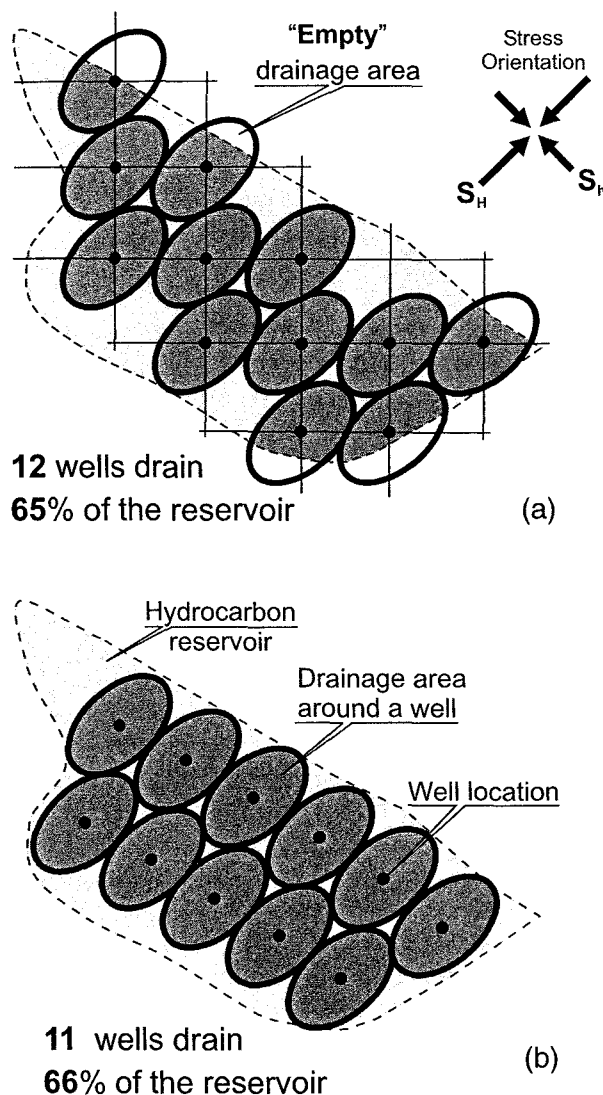
In the future, the discovery of new gigantic hydrocarbon reservoirs will be rare, thus companies will focus on the optimization of the production of existing fields. This covers exploitation of smaller reservoirs or marginal fields and activities in the deeper offshore areas. Tectonic stress in combi-

nation with the actual fracture network controls the fluid flow anisotropy and thus the drainage pattern within the reservoir. Numerous examples of a strong correlation between the preferential direction of fluid flow in a reservoir and the orientation of S_H are described by Heffer & Dowokpor (1990), Heffer & Koutsabeloulis (1995), and Heffer *et al.* (1995). Thus, knowledge about the orientation of S_H can be used for an optimized arrangement of the production wells (Fig. 10).

One distinguishes the fracture-induced permeability from the intrinsic permeability of the rock which is connected with the available pore

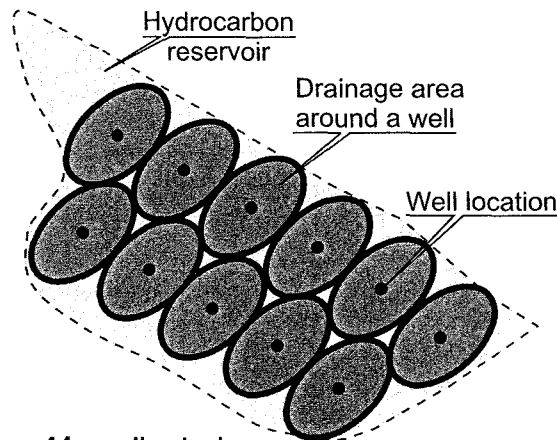
space. Both together form the effective permeability (e.g. Connolly & Cosgrove 1999). In particular, oil or gas recoveries from reservoirs with low intrinsic permeabilities require widespread networks of interconnected fractures (Lorenz *et al.* 1988; Hickman & Dunham 1992).

Oil recovery is enhanced by the creation of new (artificial) fractures (pathways). A fracture develops away from the borehole by pumping water or gels into the target area. It propagates perpendicularly to the least principal stress. Thus, advance knowledge of the stress orientations enables prediction of the orientations of stimulation fractures and thus enhances the economic success of field activities.



12 wells drain
65% of the reservoir

(a)



11 wells drain
66% of the reservoir

(b)

Fig. 10. Stress-controlled flow anisotropy (modified after Bell 1996). Due to the preferred orientation of fractures parallel to S_H , the drainage area of each well is elliptical with the long axis parallel to S_H . (a) The arrangement of wells due to geometric aspects (north-south and east-west grid) requires 12 wells for draining 65% of the reservoir. (b) The arrangement due to reservoir flow characteristic requires only 11 wells for 66% drainage and is thus more economic.

Outlook

The WSM is designed as a secure repository of stress data from academic research and economic investigations, and as a tool to work with the data. It has a long-term perspective (continuation until at least 2008) and thus enables oil companies, for example, to come back to hydrocarbon fields which had been considered as uneconomic earlier. The data are readily available via the Internet so that time-consuming searching in archives can be avoided. Additionally, with CASMO we provide a user-friendly tool for the creation of stress maps. The growth of the database by c. 20% compared with the 1997 release (1997: 9147 data sets, 2000: 10 920 data sets) justifies the hope that the data coverage on a global scale will further improve during the next few years, so that some of the large data gaps can be closed.

Stress observations are fundamental Earth science data which are used to relate global dynamic modelling of lithospheric stresses with plate movements. Other scientific challenges are the correlation between crustal dynamics and velocity anisotropies in the upper mantle, regional investigations of tectonic motions, and the comparison of stress data with modern geodetic observations as described for the Mediterranean. The increase of stress observations will promote further research projects leading to a better understanding of the sources and the effects of tectonic stresses.

Investigation of tectonic stress is not only of scientific interest, but also has an economic impact by providing information on the stability of underground openings like boreholes, tunnels, or radioactive waste depositories and thus enhances the value of the data gained by the industry. Moreover, preventing rock failure by choosing an appropriate orientation of underground openings and precautions for stabilization can be considered as a crucial security aspect for people working in mines and tunnels.

The World Stress Map project is financed by the Heidelberg Academy of Sciences and Humanities. We thank A. Becker and D. Nieuwland for their helpful and constructive reviews.

References

- ALLMENDINGER, R. W., GEPHARDT, J. W. & MARRETT, R. A. 1989. *Notes on Fault Slip Analysis*. Notes to the Geological Society of America short course 'Quantitative interpretation of joints and faults'. Cornell University, Ithaca.
- AMADEI, B. & STEPHANSSON, O. 1997. *Rock Stress and its Measurement*. Chapman & Hall, London.
- ANGELIER, J. 1984. Tectonic analysis of fault-slip data sets. *Journal of Geophysical Research*, **89**, 5835–5848.
- ANGELIER, J. & GOGUEL, J. 1979. Sur une méthode simple de détermination des axes principaux des contraintes pour une population de failles (A simple method for determining the principal axes of stress for a fault population). *Comptes Rendus de l'Académie des Sciences, Paris, Série D*, **288**, 307–310.
- ASK, M. V. S. 1998. *In-situ and laboratory stress investigations using borehole data from the North Atlantic Ocean*. PhD thesis, Department of Civil and Environmental Engineering, Royal Institute of Technology, Stockholm.
- BECKER, A. & PALADINI, S. 1990. In situ Spannungen in Nord- und Mitteleuropa. *Schriftenreihe Angewandte Geologie Karlsruhe*, **10**, 1–63.
- BECKER, A. & WERNER, D. 1994. Strain measurements with the borehole slotter. *Terra Nova*, **6**, 608–617.
- BELL, J. S. 1996. In situ stresses in sedimentary rocks (part 2): Applications of stress measurements. *Geoscience Canada*, **23**, 135–153.
- BOCK, H. 1993. Measuring in situ rock stress by borehole slotting. *Comprehensive Rock Engineering – Principles, Practice & Projects*, **3**, 433–443.
- BOCK, H. & FORURIA, V. 1983. A recoverable borehole slotting instrument for in situ stress measurements, not requiring overcoring. *Proceedings of the International Symposium on Field Measurements in Geomechanics, Zürich*, 15–29.
- BRERETON, R. & MÜLLER, B. 1991. European stress: contributions from borehole breakouts. *Philosophical Transactions of the Royal Society of London, Series A*, **337**, 165–179.
- BRUDY, M. & ZOBACK, M. D. 1999. Drilling-induced tensile wall-fractures: implications for determination of in situ stress orientation and magnitude. *International Journal of Rock Mechanics and Mining Sciences and Geomechanics Abstracts*, **36**, 191–215.
- CONNOLLY, P. & COSGROVE, J. 1999. Prediction of fracture-induced permeability and fluid flow in the crust using experimental stress data. *AAPG Bulletin*, **83**, 757–777.
- DELVAUX, D. & SPERNER, B. 2003. New aspects of tectonic stress inversion with reference to the TENSOR program. In: NIEUWLAND, D. A. (ed.) *New Insights into Structural Interpretation and Modelling*. Geological Society, London, Special Publications.
- DELVAUX, D., MOEYS, R., STAPEL, G. *et al.* 1997. Paleostress reconstruction and geodynamics of the Baikal region, Central Asia, Part 2, Cenozoic rifting. *Tectonophysics*, **282**, 1–38.
- DEMETS, C., GORDON, R. G., ARGUS, D. F. & STEIN, S. 1994. Effect of recent revisions to the geomagnetic reversal time scale on estimates of current plate motions. *Geophysical Research Letters*, **21**, 2191–2194.
- DREWES, H. 1993. A deformation model of the Mediterranean from space geodetic observations and geophysical predictions. *International Association of Geodesy, Symposium*, **112**, 373–378.
- FORDJOR, C. K., BELL, J. S. & GOUGH, D. I. 1983. Breakouts in Alberta and stress in the North American plate. *Canadian Journal of Earth Sciences*, **20**, 1445–1455.
- FUCHS, K. & MÜLLER, B. 2000. World Stress Map of the Earth: a key to tectonic processes and technological applications. *Naturwissenschaften*, **88**, 357–371.
- GORDON, R. G. & STEIN, S. 1992. Global tectonics and space geodesy. *Science*, **256**, 333–342.
- HARDCASTLE, K. C. 1989. Possible paleostress tensor configurations derived from strike-slip data in eastern Vermont and western New Hampshire. *Tectonics*, **8**, 265–284.
- HEFFER, K. J. & DOWOKPOR, A. B. 1990. Relationship between azimuths of flood anisotropy and local earth stresses in oil reservoirs. *Proceedings of the North Sea oil and gas reservoir conference*, 251–260.
- HEFFER, K. J. & KOUTSABELOULIS, N. C. 1995. Stress effects on reservoir flow; numerical modelling used to reproduce field data. In: DE HAAN, H. J. (ed.) *New Developments in Improved Oil Recovery*. Geological Society, London, Special Publications, **84**, 81–88.
- HEFFER, K. J., FOX, R. J., MCGILL, C. A. & KOUTSABELOULIS, N. C. 1995. Novel techniques show links between reservoir flow directionality, Earth stress, fault structure and geomechanical changes in mature waterfloods. *Society of Petroleum Engineers, Annual Technical Conference & Exhibition, Dallas*, SPE 30711.
- HEIDBACH, O. & DREWES, H. 2003. 3D Finite element model of major tectonic processes in the Eastern Mediterranean. In: NIEUWLAND, D. A. (ed.) *New Insights into Structural Interpretation and Modelling*. Geological Society, London, Special Publications.
- HICKMAN, R. G. & DUNHAM, J. B. 1992. Controls on the development of fractured reservoirs in the Monterey Formation of central California. In: LARSEN, R. M., BREKKE, H., LARSEN, B. T. & TELLERAAS, E. (eds) *Structural and Tectonic Modelling and its Application to Petroleum Geology*. Norwegian Petroleum Society, Special Publications, **1**, 343–353.
- JACKSON, J. & MCKENZIE, D. 1988. The relationship between plate motions and seismic tremors, and the rates of active deformation in the Mediterranean and Middle East. *Geophysical Journal of the Royal Astronomical Society*, **93**, 45–73.
- JACKSON, J., HAINES, J. & HOLT, W. 1988. The horizontal velocity field in the deforming Aegean Sea region determined from the moment tensors of earthquakes. *Journal of Geophysical Research*, **97**, 657–17 684.
- JAROSINSKI, M. 1998. Contemporary stress field distortion in the Polish part of the Western Outer Carpathians and their basement. *Tectonophysics*, **297**, 91–119.
- KANIUTH, K., DREWES, H., STUBER, K. *et al.* 1999. Crustal deformations in the central Mediterranean derived

- from the WHAT A CAT GPS project. *Proceedings of the 13th Working Meeting on European VLBI for Geodesy and Astronomy*, Wettzell, 192–197.
- KIRSCH, G. 1898. Die Theorie der Elastizität und die Bedürfnisse der Festigkeitslehre. *Zeitschrift des Vereines Deutscher Ingenieure*, **42**, 797.
- KISSEL, C. & LAJ, C. 1988. The Tertiary geodynamical evolution of the Aegean arc: a paleomagnetic reconstruction. *Tectonophysics*, **146**, 183–201.
- KISSEL, C., LAJ, C., SENGÖR, A. M. C. & POISSON, A. 1987. Paleomagnetic evidence for rotation in opposite senses of adjacent blocks in the northeastern Aegea and Western Anatolia. *Geophysical Research Letters*, **14**, 907–910.
- KLOTZ, J., ANGERMANN, D., MICHEL, G. E. *et al.* 1999. GPS-derived deformation of the central Andes including the 1995 Antofagasta $M_w = 8.0$ earthquake. *Pure Applied Geophysics*, **154**, 709–730.
- LE PICHON, X. & ANGELIER, J. 1979. The Hellenic arc and trench system: a key to the neotectonic evolution of the eastern Mediterranean area. *Tectonophysics*, **60**, 1–42.
- LE PICHON, X., CHAMOT-ROOKE, N., LALLEMANT, S., NOOMEN, R. & VEIS, G. 1995. Geodetic determination of the kinematics of central Greece with respect to Europe: Implications for eastern Mediterranean tectonics. *Journal of Geophysical Research*, **100**, 12675–12690.
- LORENZ, J. C., WARPINSKI, N. R., TEUFEL, L. W., BRANAGAN, P. T., SATTLER, A. R. & NORTHROP, D. A. 1988. Results of the Multiwell Experiment: in situ stresses, natural fractures, and other geological controls on reservoirs. *EOS Transactions, American Geophysical Union*, **69**, 817, 825–826.
- MCCLUSKY, S., BALASSANIAN, S., BARKA, A. *et al.* 2000. Global Positioning System constraints on plate kinematics and dynamics in the eastern Mediterranean and Caucasus. *Journal of Geophysical Research*, **105**, 5695–5719.
- MCKENZIE, D. P. 1970. Plate tectonics of the Mediterranean region. *Nature*, **226**, 239–243.
- MCKENZIE, D. P. 1972. Active tectonics of the Mediterranean region. *Geophysical Journal of the Royal Astronomical Society*, **30**, 109–185.
- MARDIA, K. V. 1972. *Statistics of Directional Data*. Academic Press, New York.
- MEIJER, P. TH. & WORTEL, M. J. R. 1996. Temporal variation in the stress field of the Aegean region. *Geophysical Research Letters*, **23**, 439–442.
- MERCIER, J. L., SOREL, D. & SIMEAKIS, K. 1987. Changes in the state of stress in the overriding plate of a subduction zone: the Aegean Arc from the Pliocene to the Present. *Annales Tectonicae*, **1**, 20–39.
- MÜLLER, B., ZOBACK, M. L., FUCHS, K., MASTIN, L., GREGENSEN, S., PAVONI, N., STEPHANSSON, O. & LJUNGGREN, C. 1992. Regional patterns of tectonic stress in Europe. *Journal of Geophysical Research*, **97**, 11783–11803.
- MÜLLER, B., WEHRLE, V. & FUCHS, K. 1997. The 1997 release of the World Stress Map. WWW address: <http://www.world-stress-map.org>.
- MÜLLER, B., REINECKER, J., HEIDBACH, O. & FUCHS, K. 2000. The 2000 release of the World Stress Map. WWW address: <http://www.world-stress-map.org>.
- NOOMEN, R., SPRINGER, T. A., AMBROSIUS, B. A. C. *et al.* 1996. Crustal deformations in the Mediterranean area computed from SLR and GPS observations. *Journal of Geodynamics*, **21**, 73–96.
- PESKA, P. & ZOBACK, M. D. 1995. Compressive and tensile failure of inclined wellbores and determination of in situ stress and rock strength. *Journal of Geophysical Research*, **100**, 12791–12811.
- PLUMB, R. A. & HICKMAN, S. H. 1985. Stress-induced borehole elongation: A comparison between the four-arm dipmeter and the borehole televiewer in the Auburn Geothermal well. *Journal of Geophysical Research*, **90**, 5513–5522.
- REILINGER, R. E., MCCLUSKY, S. C., ORAL, M. B. *et al.* 1997. Global Positioning System measurements of present-day crustal movements in the Arabia-Africa-Eurasia plate collision zone. *Journal of Geophysical Research*, **102**, 9983–9999.
- ROYDEN, L. 1993. The tectonic expression of slab pull at continental convergent boundaries. *Tectonics*, **12**, 303–325.
- SPERNER, B. 1996. Computer programs for the kinematic analysis of brittle deformation structures and the Tertiary tectonic evolution of the Western Carpathians (Slovakia). *Tübinger Geowissenschaftliche Arbeiten, Reihe A*, **27**, 1–120.
- SPERNER, B., RATSCHBACHER, L. & OTT, R. 1993. Fault-striae analysis: a Turbo Pascal program package for graphical presentation and reduced stress tensor calculation. *Computers & Geosciences*, **19**, 1361–1388.
- STEIN, R. S., BARKA, A. A. & DIETRICH, J. H. 1997. Progressive failure on the North Anatolian fault since 1939 by earthquake stress triggering. *Geophysical Journal International*, **128**, 594–604.
- TWISS, R. J. & UNRUH, J. R. 1998. Analysis of fault slip inversions: Do they constrain stress or strain rate? *Journal of Geophysical Research*, **103**, 12205–12222.
- WESSEL, P. & SMITH, W. H. F. 1991. Free software helps map and display data. *EOS Transactions, American Geophysical Union*, **72**, 441.
- WESSEL, P. & SMITH, W. H. F. 1998. New, improved version of the Generic Mapping Tools released. *EOS Transactions, American Geophysical Union*, **79**, 579.
- WIPIRUT, D., ZOBACK, M. D., HANSSSEN, T. H. & PESKA, P. 1997. Constraining the full stress tensor from observations of drilling-induced tensile fractures and leak-off test: Applications to borehole stability and sand production on the Norwegian margin. *International Journal of Rock Mechanics and Mining Sciences*, **34**, 417.
- ZAJAC, B. J. & STOCK, J. M. 1997. Using borehole breakouts to constrain the complete stress tensor: Results from the Siljan Deep Drilling Project and offshore Santa Maria Basin, California. *Journal of Geophysical Research*, **102**, 10083–10100.
- ZOBACK, M. D., ZOBACK, M. L., MOUNT, V. S. *et al.* 1987. New evidence on the state of stress on the San Andreas fault system. *Science*, **238**, 1105–1111.
- ZOBACK, M. L. 1992. First- and second-order patterns of stress in the lithosphere: The World Stress Map Project. *Journal of Geophysical Research*, **97**, 11703–11728.